Jordanian Journal of Computers and Information Technology (JJCIT), Vol. 2, No. 1, April 2016.

A LOW COMPLEXITY DIRECTION FINDING SYSTEM BASED ON A SIX-PORT INTEGRATED MIMO ANTENNA SYSTEM

Rifaqat Hussain[1], Ali H. Muqaibel[2], Wajih Abu-Al-Saud[3] and Mohammad S. Sharawi[4]

Electrical Engineering Department, King Fahd University for Petroleum and Minerals (KFUPM), Dhahran 31261 Saudi Arabia

{rifaqat[1], muqaibel[2], wajih[3], msharawi[4]}@kfupm.edu.sa

(Received: 15-Dec.-2015, Revised: 28-Jan.-2016, Accepted: 03-Feb.-2016)

ABSTRACT

In this paper, a low complexity microwave based direction finding (DF) system is presented. The proposed system consists of a single six-port (SP) circuit integrated with a reconfigurable multiple-input-multiple-output (MIMO) antenna system. The SP circuit covers a wide frequency band (1.68-2.25 GHz). The SP circuit is also characterized for phase error compensation caused by the slight asymmetry of SP and power detectors. The reconfigurable MIMO antenna system used is a compact design and covers several well-known wireless standards in the frequency bands from 0.7 GHz to 3 GHz. The SP circuit is integrated with the reconfigurable MIMO antenna system to form a complete beam forming mode for second generation cognitive radio (CR) platforms. The proposed design is a complete integrated solution with DF capabilities for CR platforms. The design is suitable to be used in compact wireless handheld and mobile communication devices. The fabricated integrated system achieves ±16^o accuracy in its direction of arrival estimates.

KEYWORDS

Microwave DF, Six-port circuit, Beamforming mode, Reconfigurable MIMO antenna, Cognitive radio platforms.

1. INTRODUCTION

Low complexity direction finding (DF) systems in wireless communication devices have attracted increasing attention over the past decade. Radio frequency (RF) based DF schemes are of particular interest, because of their low profile RF structure and their minimal data processing requirements. RF DF schemes are gaining popularity in wireless communication devices and in military services. Wireless handheld devices complying with 3G/4G wireless standards integrated with RF DF systems would be an attractive feature for next generation cognitive radio (CR) platforms [1].

The basic concept of RF DF is an angle-of-arrival (AoA) estimation of an incoming RF signal from a distant source. Classical techniques of digital signal processing (DSP) algorithms, such as Multiple Signal Classification (MUSIC) and Estimation of Signal Parameters via Rotational Invariance Technique (ESPRIT), use an array of antennas followed by multiple receivers to estimate the AoA [2]-[3]. With the use of such single or multiple receivers, computationally intensive DF algorithms and techniques are limited to be used in practical wireless handheld and mobile devices [4]. RF DF systems using the six-port (SP) circuit have gained popularity over the past few years, because of their low cost and simple microwave structure [5].

Most of the existing 3G/4G wireless standards cover low frequency bands, while most of the existing SP structures cover frequency bands above 2GHz [5]–[7]. In addition to high frequency operation, the given SP circuit dimensions are not suitable to be used in wireless handheld devices. A low frequency compact SP circuit was presented in [8]. Although the SP design was compact and covered low frequency bands, it was not presented in a complete integrated solution for AoA estimation. Also, a dual SP design was presented in [9] with low frequency operation. In [10], an ultra-wideband (UWB) six-port network was presented with operating bands of 2~8 GHz. It consisted of a Wilkinson power divider and three 3-dB quadrature couplers. The fabricated SP phase measurement system with calibration technique based on support vector regression (SVR) was introduced. Results show that when the SVR model was efficiently utilized, a phase error of ±1.5274^{o}was obtained.

In this work, we propose a complete integrated solution complying with the second generation CR standards in mobile devices. The system integrates a compact SP circuit based on [8] with a reconfigurable MIMO antenna system based on [11]. The antenna system used covers several frequency standards in the frequency bands from 0.7 to 3 GHz, while the SP circuit used covers frequency bands from 1.68 to 2.25 GHz. The unique feature of the proposed design is the integration of the SP circuit with the reconfigurable MIMO antenna system for lower frequency bands of operation. The complete system was tested and its AoA determination capability was studied in a complete experimental setup.

Moreover, the integrated design is easily distinguished from all other contemporary designs, as it could be utilized in wireless handheld devices and mobile terminals. Additionally, the complete system can be used in data Tx/Rx mode and beam forming mode complying with second generation CR standards.

2. DF IN COGNITIVE RADIO PLATFORMS

The revolutionary technique of CR is defined as a system with efficient utilization of frequency spectrum along with direction finding capabilities [1]. In this section, the classification of CR antennas, their use in beamforming mode and operating principles are discussed.

2.1 Beamforming in CR Platforms

Front-end antennas for CR platforms are categorized as shown in Figure 1. CR antennas consist of two types of antennas: (1) an ultra-wide-band (UWB) sensing antenna and (2) a reconfigurable communication antenna. Reconfigurable antennas can be utilized to change their operating fundamental characteristics; i.e., resonance frequency, radiation pattern, polarization and impedance bandwidth. Reconfigurable antennas can be simple frequency reconfigurable ones or reconfigurable MIMO antennas that can be utilized to enhance the data rate capability. The MIMO antenna system can be used in two modes of operation in a CR platform: (1) Data Tx/Rx mode and (2) Beamforming mode. Beamforming mode in CR platforms can be utilized for RF DF.

2.2 DF Operating Principle

The block diagram of the operating principle of AoA estimation based on RF DF using the SP circuit is shown in Figure2. The detailed description of the operating principle of the SP circuit for RF DF is given in detail in [8]. The receiving antennas are separated by distance d with a path difference Δd, while the received signals experience a phase difference $\Delta\phi$. AoA (ϕ) of a distant object can be calculated using Δd and $\Delta\phi$ information using Equation (1), where λ is the wave length of operating frequency.

$$\Delta d = \lambda \frac{\Delta \emptyset}{2\pi}, \ \sin \emptyset = \frac{\lambda}{d} \frac{\Delta \emptyset}{2\pi} \quad (1)$$

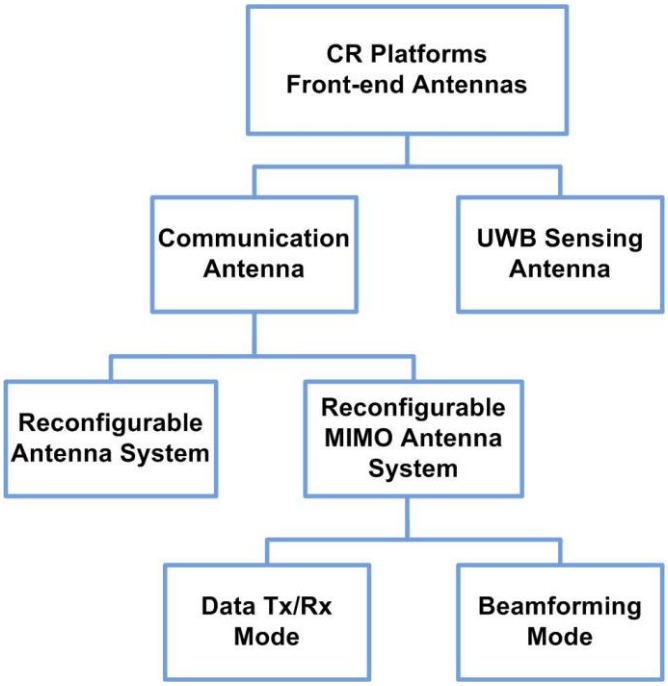

Figure 1. Classification of CR antennas.

Equation (1) can be used to determine the AoA of the incoming RF signal based on the information of phase difference. The SP circuit is fed with incoming wave signals from the antennas and used to find the phase difference. Once the phase difference becomes known, it could be utilized to find the AoA of distant target objects.

2.3 SP Operating Principle

In this sub-section, the operating principle of RF DF using SP circuit is described. Two input RF signals a_5 and a_6 are received by two antennas separated by distance *d*. The two signals are impinging on the SP circuit with phase difference $\Delta\phi$ owing to path difference Δd. The phase difference can be written as $\Delta\phi = \phi_6 - \phi_5$. The complete details of the SP circuit for RF DF are discussed in [9]. The SP circuit used in this experimentation is shown in Figure 3. The SP circuit output scan be written as:

$$b_i = a_5 . S_{5i} + a_6 . S_{6i} \tag{2}$$

The resultant signal at output port-1 can be written as:

$$b_1 = \frac{a}{2} . e^{\left(j\left[\emptyset_5 - \frac{\pi}{2}\right]\right)} \left\{1 + \alpha e^{[j(\Delta\emptyset + \pi)]}\right\} \tag{3}$$

For port-2, the resultant signal is given by:

$$b_2 = \frac{-a}{2} . e^{(j[\emptyset_5])} \left\{1 + \alpha e^{\left[j\left(\Delta\emptyset + \frac{\pi}{2}\right)\right]}\right\} \tag{4}$$

Similarly, for port-3, the resultant signal is:

$$b_3 = \frac{-a}{2} . e^{(j[\emptyset_5])} \left\{1 + \alpha e^{[j(\Delta\emptyset)]}\right\} \tag{5}$$

Similarly, for port 4:

$$b_4 = \frac{-a}{2} . e^{\left(j\left[\emptyset_5 + \frac{\pi}{2}\right]\right)} \left\{1 + \alpha e^{\left[j\left(\Delta\emptyset - \frac{\pi}{2}\right)\right]}\right\} \tag{6}$$

"A Low Complexity Direction Finding System Based on a Six-port Integrated MIMO Antenna System", Rifaqat Hussain, Ali H. Muqaibel, Wajih Abu-Al-Saud and Mohammad S. Sharawi.

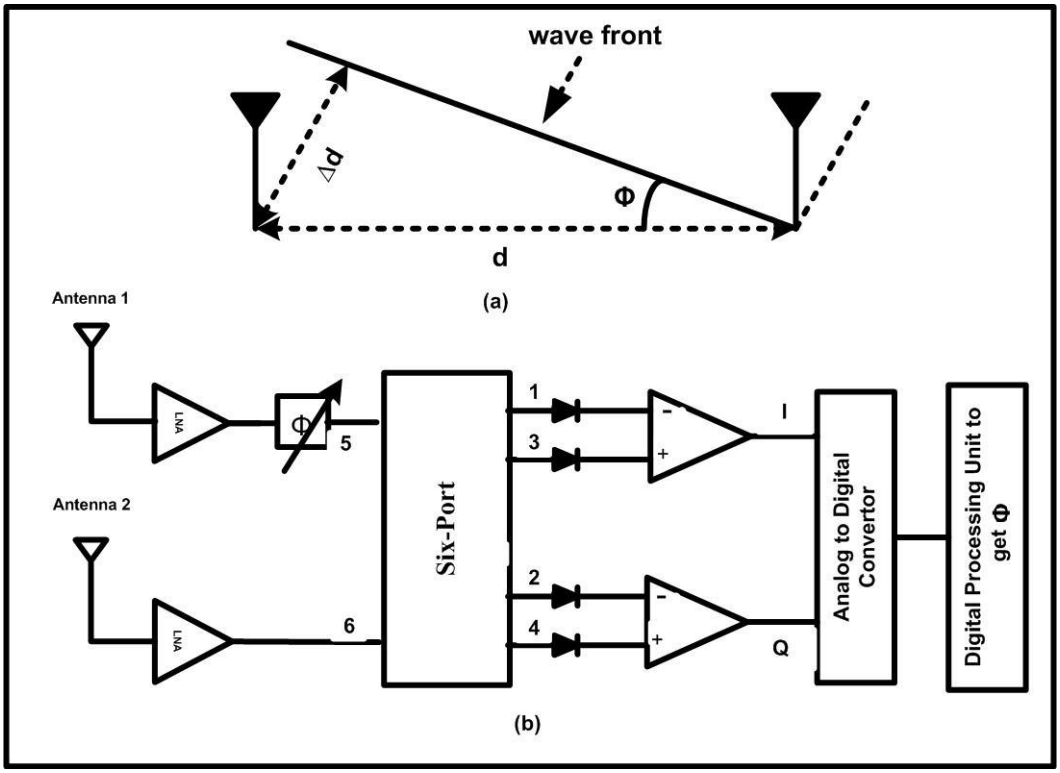

Figure 2. Six-port based direction finding system.

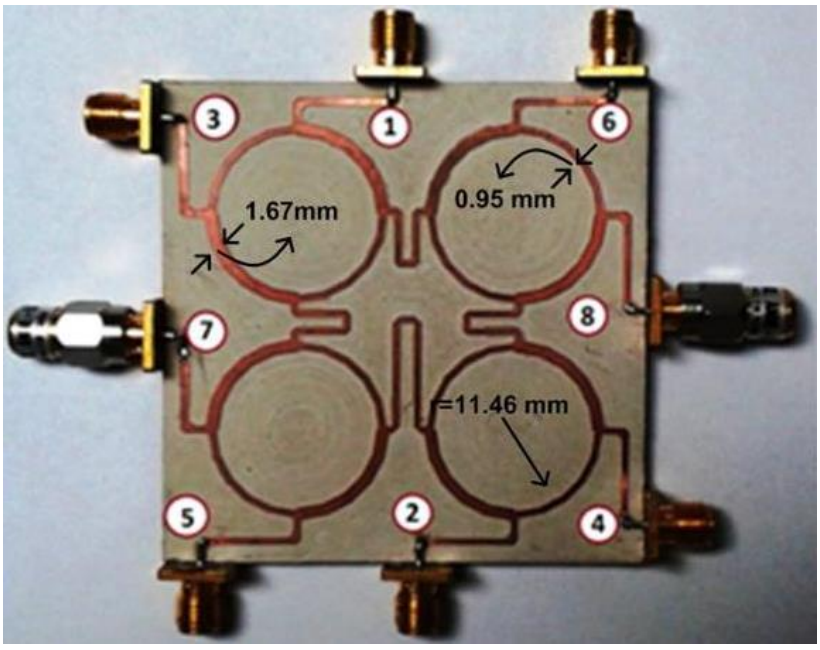

Figure 3.Single SP circuit [8].

The SP output RF signals are passed through power detectors and can be written as:

$$V_i = K_i|b_i|^2 \quad (7)$$

$$i=1,2,3,4$$

where K_i constants are measured in V/W. The constants are specified for each power detector showing the relationship between output voltage and input power. Each output of the power detector circuit is passed through a differential amplifier circuit to get the two components in-phase and quadrature (I and Q) [9]. For the SP, these are I and Q.

$$I = V_3 - V_1 = \alpha K a^2 . \cos(\Delta\emptyset) \tag{8}$$

$$Q = V_4 - V_2 = \alpha K a^2 . \sin(\Delta\emptyset) \tag{9}$$

The vector Γ is defined for the dual SP in terms of the in-phase and quadrature components as:

$$\Gamma = I + jQ = K . a^2 . \exp(j\Delta\emptyset) \tag{10}$$

where a is the amplitude of the incoming RF signal and α is the ratio a_6/a_5. Equation (10) can be used to determine the phase relationship between the input RF signals. The measured $\Delta\phi$ can be used in Equation (1) to find the AoA (ϕ) of the distant target object.

3. CHARACTERIZATION OF THE SIX-PORT OUTPUTS

The direction of the incoming RF waves can be easily determined using Equation (1) based on the determination of the phase differences measured by the SP given in Equation (10). But this calculation overlooks the phase error caused by the slight asymmetry of the various SP paths, asymmetry of the power detectors, as well as frequency measurement errors. These errors in the phases were characterized via simulations and by laboratory measurements. In this section, a mathematical analysis is carried out to develop an analytical model to compensate for these errors in order to get high accuracy in phase measurement at the output of each port.

$$\emptyset'_{5i} = phase\ error\ at\ output\ port\ i\ due\ to\ input\ port\ 5, where\ i = 1,2,3,4;$$
$$\emptyset'_{6i} = phase\ error\ at\ output\ port\ i\ due\ to\ input\ port\ 6, where\ i = 1,2,3,4 \tag{11}$$

So, the output signal can be written as a linear combination of input signals a_5 and a_6.

$$b_1 = a_5 . S_{51} + a_6 . S_{61}$$

$$b_1 = a . e^{j\emptyset_5} . e^{j\emptyset'_{51}} - \frac{j}{2} + \alpha a_5 . \frac{j}{2} e^{j\Delta\emptyset}\ e^{j\emptyset'_{61}}$$

$$b_1 = \frac{a}{2} . e^{j\left[\emptyset_5 - \frac{\pi}{2}\right]} . e^{j\emptyset'_{51}} + \alpha . a \frac{j}{2} e^{j\emptyset_5}\ e^{j\Delta\emptyset}\ e^{j\emptyset'_{61}}$$

$$b_1 = \frac{a}{2} . e^{\left(j\left[\emptyset_5 - \frac{\pi}{2}\right]\right)} \left\{ e^{j\emptyset'_{51}} + \alpha e^{[j(\Delta\emptyset+\pi)]} e^{j\emptyset'_{61}} \right\}$$

$$b_1 = \frac{a}{2} . e^{\left(j\left[\emptyset_5 - \frac{\pi}{2}\right]\right)} \left\{ 1 + \alpha e^{[j(\Delta\emptyset+\pi)]}\ \frac{e^{j\emptyset'_{61}}}{e^{j\emptyset'_{51}}} \right\}$$

$$b_1 = \frac{a}{2} . e^{\left(j\left[\emptyset_5 - \frac{\pi}{2}\right]\right)} e^{j\emptyset'_{51}} \left\{ 1 + \alpha e^{[j(\Delta\emptyset+\pi)]}\ e^{j\Delta\emptyset'_1} \right\} \tag{12}$$

$$b_2 = a_5 . S_{52} + a_6 . S_{62}$$

$$b_2 = \frac{a}{2} . e^{j\emptyset_5} . e^{j\emptyset'_{52}} - 1 + \alpha a_5 . \frac{-j}{2} e^{j\Delta\emptyset} . e^{j\emptyset'_{62}}$$

$$b_2 = \frac{-a}{2} . e^{(j[\emptyset_5])} e^{j\emptyset'_{52}} \left\{ 1 + \alpha e^{\left[j\left(\Delta\emptyset + \frac{\pi}{2}\right)\right]}\ e^{j\Delta\emptyset'_2} \right\} \tag{13}$$

$$b_3 = a_5.S_{53} + a_6.S_{63}$$

$$b_3 = \frac{-a}{2}.e^{j\emptyset_5}.e^{j\emptyset'_{53}} - 1 + \alpha a_5.\frac{-1}{2}e^{j\Delta\emptyset}.e^{j\emptyset'_{63}}$$

$$b_3 = \frac{-a}{2}e^{j[\emptyset_5]} + \alpha a\frac{-1}{2}\ e^{j\emptyset_5}e^{j\Delta\emptyset}$$

$$b_3 = \tfrac{-a}{2}.e^{(j[\emptyset_5])}\ e^{j\emptyset'_{53}}\left\{1 + \alpha e^{[j(\Delta\emptyset)]}\ e^{j\Delta\emptyset'_3}\right\} \quad (14)$$

$$b_4 = a_5.S_{54} + a_6.S_{64}$$

$$b_4 = \frac{-j}{2}a.e^{(j[\emptyset_5])}.e^{j\emptyset'_{64}} + \alpha a\frac{-1}{2}\ e^{j\emptyset_5}\ e^{j\Delta\emptyset}.e^{j\emptyset'_{64}}$$

$$b_4 = \frac{-a}{2}e^{(j[\emptyset_5+\frac{\pi}{2}])}.e^{j\emptyset'_{64}} + \alpha a\frac{1}{2}\ e^{j\emptyset_5}\ e^{j\Delta\emptyset} - j.-j.e^{j\emptyset'_{64}}$$

$$b_4 = \tfrac{-a}{2}e^{(j[\emptyset_5+\frac{\pi}{2}])}.e^{j\emptyset'_4}\ \left\{1 + \alpha e^{\left[j\left(\Delta\emptyset - \frac{\pi}{2}\right)\right]}\ e^{j\Delta\emptyset'_4}\right\} \quad (15)$$

Supposing that four identical detectors (K_i = K) are used, the dc output voltages including the error terms become:

$$V_1 = K_1|b_1|^2 = K\tfrac{a^2}{4}[1 + \alpha^2 - 2\alpha.\cos(\Delta\emptyset + \Delta\emptyset'_1)] \quad (16)$$

$$V_2 = K_2|b_2|^2 = K\tfrac{a^2}{4}[1 + \alpha^2 - 2\alpha.\sin(\Delta\emptyset + \Delta\emptyset'_2)] \quad (17)$$

$$V_3 = K_3|b_3|^2 = K\tfrac{a^2}{4}[1 + \alpha^2 + 2\alpha.\cos(\Delta\emptyset + \Delta\emptyset'_3)] \quad (18)$$

$$V_4 = K_4|b_4|^2 = K\tfrac{a^2}{4}[1 + \alpha^2 + 2\alpha.\sin(\Delta\emptyset + \Delta\emptyset'_4)] \quad (19)$$

where

$$\Delta\emptyset'_1 = \emptyset'_{61} - \emptyset'_{51}$$
$$\Delta\emptyset'_2 = \emptyset'_{62} - \emptyset'_{52}$$
$$\Delta\emptyset'_3 = \emptyset'_{63} - \emptyset'_{53}$$
$$\Delta\emptyset'_4 = \emptyset'_{64} - \emptyset'_{54}$$

In the *I/Q* complex plane, a Γ vector can be defined using the four six-port DC output voltages with error terms. The error terms are known a prior and can be used to adjust or compensate for errors to give high precision in phase measurement.

Once the error in each phase of the SP is characterized, the error in the incoming RF wave can be analyzed based on Equations (16)–(19). This phase error in each path can be compensated for using an additional phase compensation block to have more accurate DF results. This block could be implemented in hardware using a field programmable gate array (FPGA) or software based-phase compensation can produce satisfactory results.

4. SP CIRCUIT INTEGRATION WITH THE RECONFIGURABLE MIMO ANTENNA SYSTEM

The complete measurement setup of an RF DF consists of a transmitting antenna as a source and a receiving MIMO antenna system integrated with SP circuit for AoA estimation.

Jordanian Journal of Computers and Information Technology (JJCIT), Vol. 2, No. 1, April 2016.

4.1 Reconfigurable MIMO Antenna System

The receiving antenna used was a reconfigurable modified PIFA MIMO antenna system along with its UWB sensing antenna as shown in Figure 4. The complete antenna system consists of two printed circuit boards with main board dimensions of 65×120×1.56 mm^3. The bottom layer consisted of the UWB sensing antenna. The secondary elevated board contained the reconfigurable antenna that was short-circuited with GND plane. The complete antenna system was realized on a commercial FR-4 substrate with ε_r=4.4 [11].

Each MIMO antenna element was embedded with two PIN diodes. The diodes were used for discontinuity of the antenna structure. The diodes were used to provide more flexibility by their ON/OFF operation for the various antenna radiating structures. The two PIN diodes in each antenna element resulted in four distinct operating modes for each MIMO antenna element. The various modes were used to resonate the antenna at various bands to cover particular wireless standards [11].

4.2 Measurements Setup

To find the AoA from a distant source, a reconfigurable MIMO antenna system integrated with a single SP circuit was used. The source used was an UWB antenna. A reconfigurable MIMO antenna system was used as the receiving system. Figure 5 shows an overview of the implemented system. The receiving antennas (within the MIMO antenna system) were separated by a distance of 53 mm (centre to centre). Owing to the path difference between the two receiving antennas, the propagated signal had a shift that was utilized to find the AoA.

4.3 Details of the Receiver Setup

A detailed view of the measurement setup at the receiving side is shown in Figure 6. The receiving antenna used is a two-element reconfigurable MIMO antenna system. The antenna operates at four distinct modes covering several frequency bands. The details of each mode and its operating frequencies were completely described in [11]. In the current scenario, we have used it in mode-1 and mode-4 at frequency bands 2020 MHz and 1690 MHz. The proposed SP circuit covered frequency ranges starting from 1.68 GHz to 2.25 GHz. The two reconfigurable antennas were connected with low noise amplifiers (LNA). The LNA used was the ZX60-33LN-S+, with a wide bandwidth covering frequency bands from 50~3000MHz. Its gain was between 13 ~ 14.4 dB in the frequency range between 1690~2020MHz.

The output of the LNA was fed to the SP circuit at port-5 and port-6. Two ports of the SP circuit were terminated with 50Ω loads. The four output ports of the SP structure were connected with the power detectors (ZX47-40LN-S+) followed by a difference amplifier based on the LM 741 IC. The output of the SP was passed through a power detector to get the DC signal. The power detector covered a wide range with low noise DC output and needed a single 5V supply. The outputs of the difference amplifiers were the in-phase (*I*) and quadrature (*Q*) components. Both (*I*) and (*Q*) were DC and were acquired by a data acquisition card (LabJack u6). Two channels were used for acquiring this data. The data acquired by the data acquisition system were processed in MATLAB for AoA estimation using Equation (1). Figure 7 shows all the components of the measurement setup. Figure 7(a) shows the source, while Figure 7(b) shows the setup used for the direction of the source. Figure 7(c) shows the SP circuit integrated with the MIMO antenna system, while Figure 7(d) shows the LabJack u6 interface for data acquisition.

"A Low Complexity Direction Finding System Based on a Six-port Integrated MIMO Antenna System", Rifaqat Hussain, Ali H. Muqaibel, Wajih Abu-Al-Saud and Mohammad S. Sharawi.

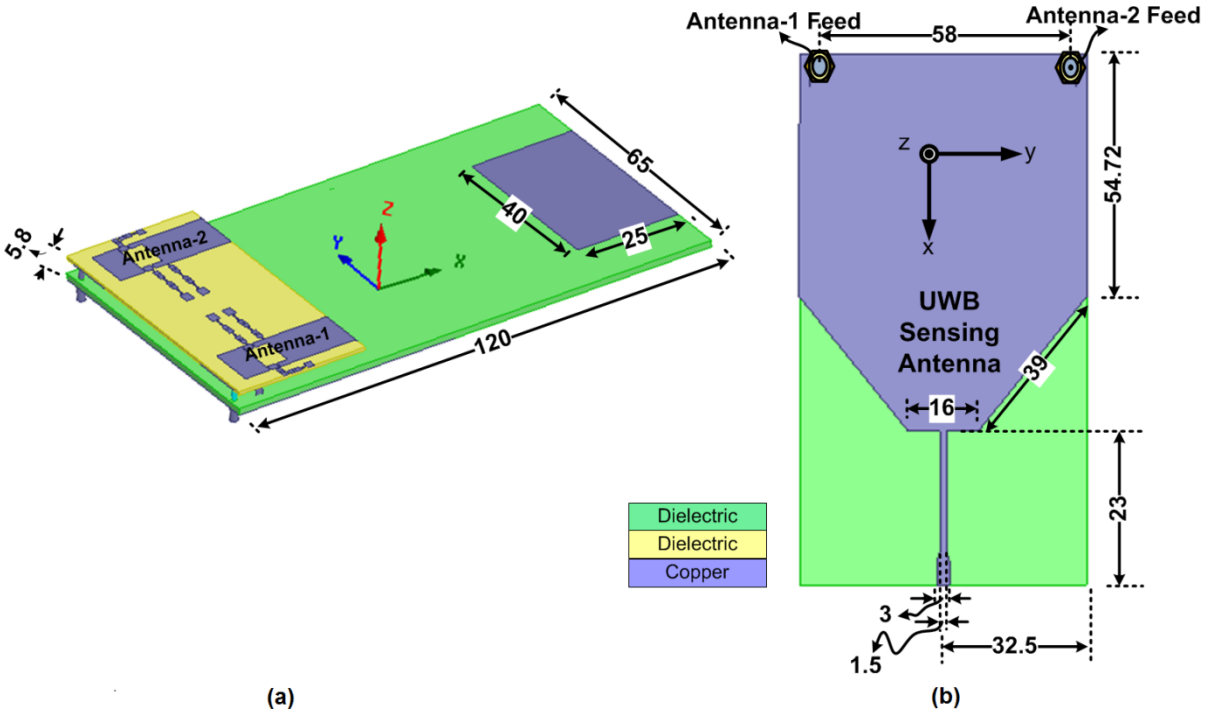

Figure 4.Reconfigurable MIMO antenna system (a) Top view (b) Bottom view. [11] - All dimensions are in mm.

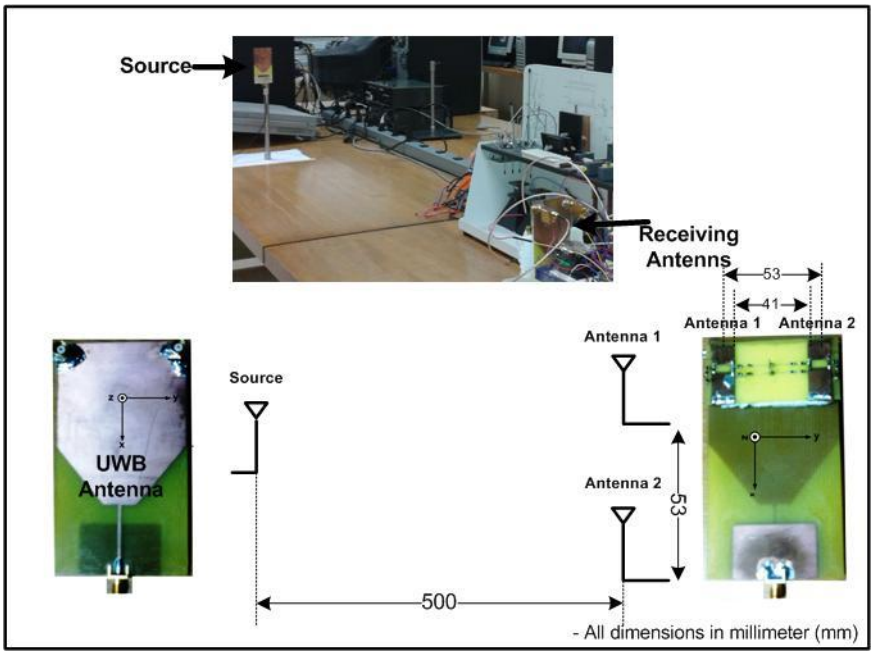

Figure 5.Block diagram of the DF measurement setup.

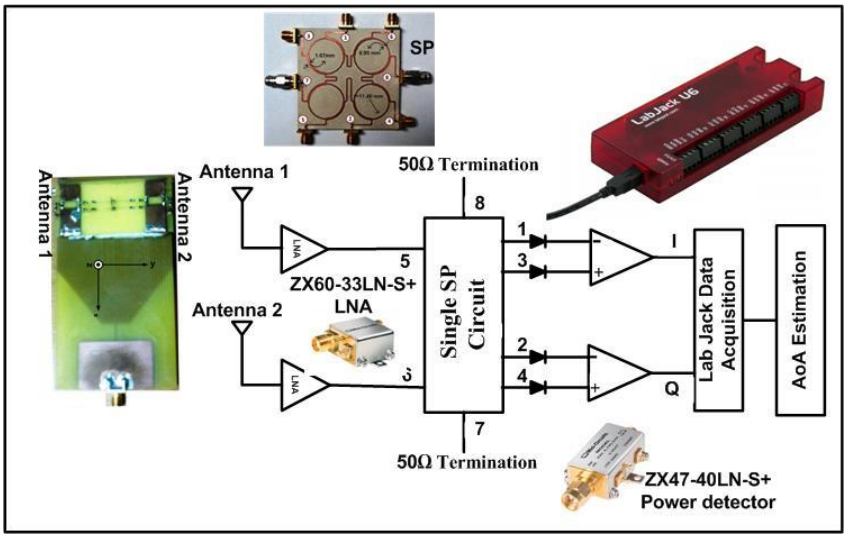

Figure 6. Detailed view of SP integration with reconfigurable MIMO antenna system for RF DF.

5. MEASUREMENT RESULTS

In the setup shown in Figure 7, a single SP circuit was used to determine the AoA in 2D. Using a single SP with a two-element antenna setup can be used to determine the AoA in a single plane. For a complete 3D (i.e., θ and ϕ) DF, a dual SP circuit with four antenna elements is required. Due to hardware limitations, in this work we have determined the AoA in 2D only.

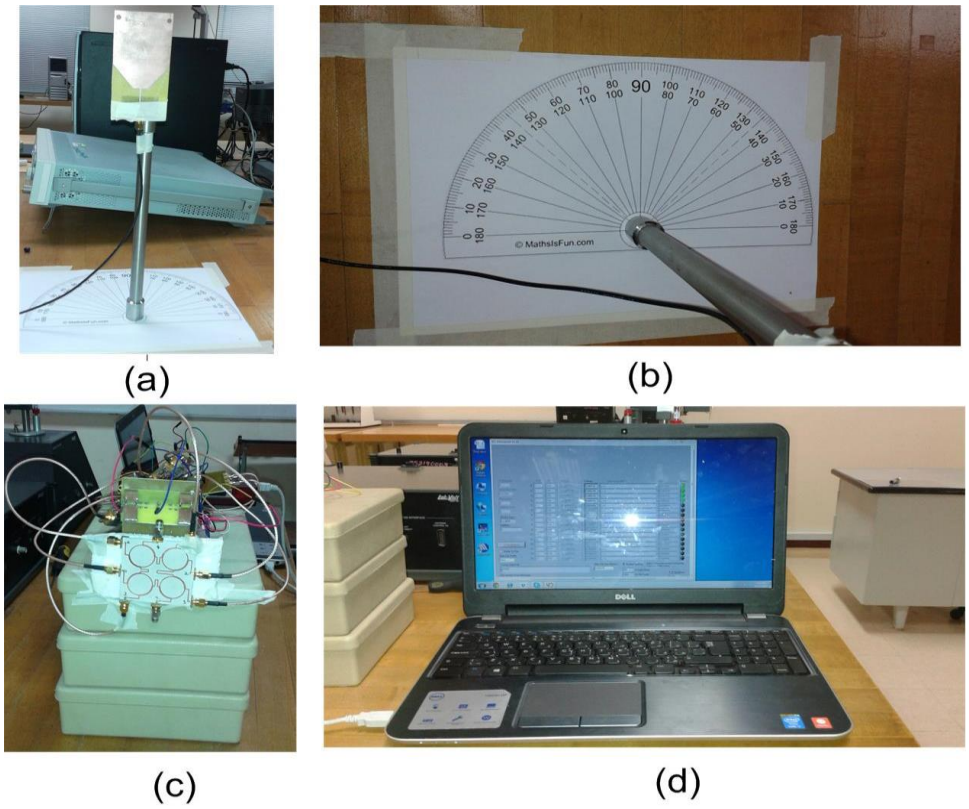

Figure 7. (a) RF source (b) Setup for angle adjustment (c) SP circuit integrated with a two-MIMO antenna system (d) LabJack interface for data acquisition.

5.1 Description of AoA Measurements

The objective of this work was to find the AoA of an RF distant source using the SP circuit integrated with reconfigurable MIMO antenna system. In this experiment, AoA measurements were made under known conditions. The receiving antenna was located with known orientation. The AoA of the incoming signal wave was known beforehand. A single antenna was positioned at known angles with respect to the receiver. The receiving antenna was operated with a single tone signal at 1690 MHz and 2020 MHz for two different measurements of AoA determination. This experiment was conducted at the Microwave Lab at KFUPM. In this AoA experiment, the transmitting and receiving antennas were placed at a distance of 500 mm. The distance was made to ensure the minimum level of power to be received for accurate AoA estimation. The orientation of the transmitting antenna was changed for azimuth angles between ±80º. It has been found that the error was becoming drastic for angles above ±60º. The maximum errors found in the AoA measurements for azimuth angle between ±60º were 16º and 13º for frequency bands1690 MHz and 2020 MHz, respectively. The error introduced in the phase by the SP was subtracted from the final error plots (the phase response of the SP was obtained from the measured parameters). Figures 8 and 9 show the error in the estimated AoA($\tilde{\phi}$) based on the measured values of (I) and (Q) using Equation (1) for the frequency bands 1690 MHz and 2020 MHz. The figures show the error in estimated AoA ($\tilde{\phi}$). Practically, with the current setup of SP and two-element MIMO antenna, the feasible range of scanning angle is from -60º to 60º with a maximum phase error in estimated AoA ($\tilde{\phi}$) of 16º in the given two bands of operation.

5.2 Sources of Error in AoA Estimation

The proposed design was able to estimate the AoA with a maximum error of ±16º. Although, the error was high, it helps in understanding the problem and its implementation. The possible sources of error are:

1. Ideally, the antenna elements are supposed to be 0.5λ apart. The accuracy of the results drops for closely spaced antenna elements. In the current scenario, the two antennas are separated by a distance of 0.23λ and 0.27λ, for the two frequency bands of 1690 MHz and 2020 MHz, respectively.
2. Although all the circulators in the SP were designed to be symmetrical in the SP design, due to fabrication tolerances, some phase error was observed at the output of SP circuit and this contributes to the final estimated error.
3. Asymmetry and non-linearities resulting from the power detectors and difference amplifies contributed to phase errors as well.
4. Different circuit modules were connected using wires. The slight difference in the lengths of wires might have added extra phase, thus contributing to this final error.

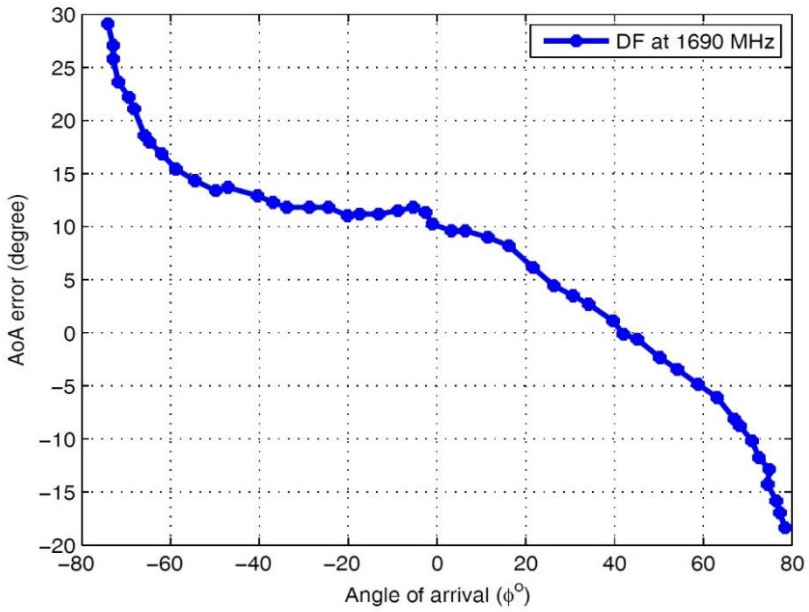

Figure 8.Angle of arrival at 1690 MHz.

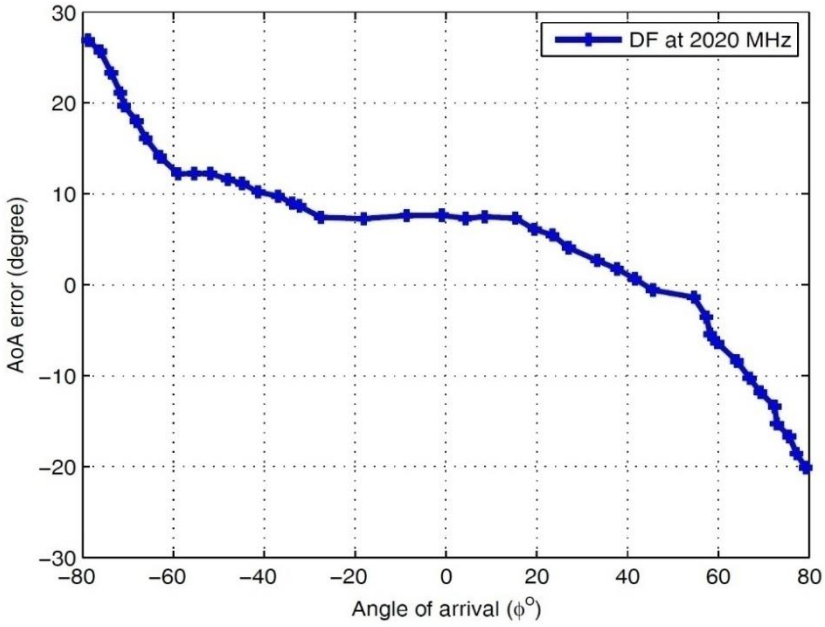

Figure 9.Angle of arrival at 2020 MHz.

6. CONCLUSIONS

In this paper, a low profile RF DF system is proposed for second generation CR applications. The complete integrated system is of low cost, targeting lower frequency bands of practical wireless devices and could be utilized for low processing DF systems in wireless handheld devices and mobile terminals. The compact single SP circuit integration with the multi-band reconfigurable MIMO antenna system is unique due to its contemporary design for RF DF. The complete system is versatile, as it could be utilized to enhance the data throughput as well as in beam forming mode for AoA estimation. The maximum error observed using this complete system was ±16 °.

ACKNOWLEDGEMENTS

This project was funded by the National Plan for Science, Technology and Innovation (Maarifah) - King Abdul Aziz City for Technology- through the Science and Technology Unit at King Fahd University of Petroleum and Minerals (KFUPM), Kingdom of Saudi Arabia; award number 12-ELE3001-04.

REFERENCES

[1] J. Bernhard, J. Reed, J. Park, A. Clegg, A. Weisshaar and A. Abouzeid,"Final Report of the National Science Foundation Workshop on Enhancing Access to the Radio Spectrum (EARS),"Arlington, Virginia, 4-6August 2010.

[2] R. Schmidt, "Multiple Emitter Location and Signal Parameter Estimation," IEEE Transactions on Antennas and Propagation, vol. 34, no. 3, pp.276–280, 1986.

[3] R. Roy and T. Kailath, "Esprit-estimation of Signal Parameters via Rotational Invariance Techniques," IEEE Transactions on Acoustics, Speech and Signal Processing, vol. 37, no. 7, pp. 984–995, 1989.

[4] D. Peavey and T. Ogumfunmi, "The Single Channel Interferometer Using a Pseudo-doppler Direction Finding System," in IEEE International Conference on Acoustics, Speech and Signal Processing, vol. 5, pp. 4129–4132, 1997.

[5] G. Vinci, F. Barbon, B. Laemmle, R. Weigel and A. Koelpin, "Wide Range Dual Six-Port Based Direction-of-arrival Detector," in IEEE 7thGerman Microwave Conference (GeMiC), pp. 1–4, 2012.

[6] S. Tatu, K. Wu and T. Denidni, "Direction-of-arrival Estimation Method Based on Six-port Technology," IEE Proceedings-Microwaves, Antennas and Propagation, vol. 153, no. 3, pp. 263–269, 2006.

[7] H. Peng, Z. Yang and T. Yang, "Design and Implementation of a Practical Direction Finding Receiver," Progress in Electromagnetic Research Letters, vol. 32, pp. 157–167, 2012.

[8] R. Hussain and M. S. Sharawi, "Compact Low Frequency Six-port Design for Wireless Communication Devices,"17th IEEE Mediterranean Electrotechnical Conference (MELECON), pp. 29-32, 13-16 April 2014.

[9] R. Hussain and M. S. Sharawi, "A Dual Six-port with Two-angle Resolution and Compact Size for Mobile Terminals," in IEEE Radio and Wireless Symposium (RWS), pp. 226–228, 2014.

[10] H. Peng, Y. Ziqiang Yang and T. Yang, "Design and Implementation of an Ultra-wideband Six-port Network," Progress in Electromagnetics Research 131, pp. 293-310, 2012.

[11] R. Hussain and M. S. Sharawi, "Integrated Reconfigurable Multiple-input–multiple-output (MIMO) Antenna System with an Ultra-wideband Sensing Antenna for Cognitive Radio Platforms," IET Microwaves, Antennas and Propagation, vol. 9, no. 9, pp. 940-947, 2015.

[12] S. O. Tatu, E. Moldovan, K. Wu, R. G. Bosisio and T. A. Denidni, "Ka Band Analog Front-end for Software-defined Direct Conversion Receiver," IEEE Transactions on Microwave Theory and Techniques, vol. 53,no. 9, pp. 2768–2776, 2005.

Jordanian Journal of Computers and Information Technology (JJCIT), Vol. 2, No. 1, April 2016.

ملخص البحث:

في هذا البحث، يتم تقديم نظام منخفض التعقيد لإيجاد الاتجاه في نطاق الميكروويف. النظام المقترح يتكون من دائرة مفردة سداسية المنافذ، مدمجة مع نظام هوائيات متعدد المداخل- متعدد المخارج قابل لإعادة التشكيل. تغطي الدائرة سداسية المنافذ نطاقاً ترددياً واسعاً (1.68- 25.2 جيجاهيرتز). كذلك تم وصف خصائص الدائرة سداسية المنافذ لتعويض خطأ الطور الناجم عن عدم التجانس الطفيف للمنافذ الستة وكواشف القدرة. نظام الهوائيات متعدد المداخل- متعدد المخارج القابل لإعادة التشكيل المستخدم في هذا البحث ذو تصميم مدمج، ويغطي عدة مقاييس معروفة جيداً في مجال الاتصالات اللاسلكية في النطاقات الترددية من 0.7 جيجاهيرتز إلى 3 جيجاهيرتز.

لقد تم دمج الدائرة سداسية المنافذ مع نظام الهوائيات متعدد المداخل- متعدد المخارج القابل لإعادة التشكيل لتشكيل نسق كامل لتكوين الشعاع للجيل الثاني من منصّات الرّاديو المدرَكة. والتصميم المقترح هو حلّ متكامل يمتلك القدرة على إيجاد الاتجاه لمنصّات الرّاديو المدرَكة.

والجدير بالذكر أنّ التصميم المقترح مناسب للاستخدام في أجهزة الاتصال اللاسلكية المدمجة المحمولة باليد و النقّالة. ويحقق النظام المدمج المُصنّع دقةً في تقدير اتجاه الإشارات المستقبلية في حدود ± 16°.